

Tuning surface metallicity and ferromagnetism by hydrogen adsorption at the polar ZnO(0001) surface

N. Sanchez, S. Gallego, J. Cerdá and M.C. Muñoz*
*Instituto de Ciencia de Materiales de Madrid, Consejo Superior
de Investigaciones Científicas, Cantoblanco, 28049 Madrid, Spain*
(Dated: December 4, 2018)

The adsorption of hydrogen on the polar Zn-ended ZnO(0001) surface has been investigated by density functional *ab-initio* calculations. An on top H(1×1) ordered overlayer with genuine H-Zn chemical bonds is shown to be energetically favorable. The H covered surface is metallic and spin-polarized, with a noticeable magnetic moment at the surface region. Lower hydrogen coverages lead to strengthening of the H-Zn bonds, corrugation of the surface layer and to an insulating surface. Our results explain experimental observations of hydrogen adsorption on this surface, and not only predict a metal-insulator transition, but primarily provide a method to reversible switch surface magnetism by varying the hydrogen density on the surface.

PACS numbers: 71.20.Tx, 73.22.-f, 71.70.Ej

ZnO is one of the most technologically important metal oxides, which holds great promise for applications as a wide band gap semiconductor: it shows the largest charge-carrier mobility among oxides, extraordinary catalytic properties and the unusual coexistence of transparency and conductivity [1]. The recently reported high temperature (HT) ferromagnetism in ZnO-based thin layers and nanostructures [2] turns it additionally into a potential HT semiconducting ferromagnet, which could be used in magnetoelectric and magnetotransport devices tuning simultaneously charge and spin [3]. However, at present, and despite numerous experimental and theoretical studies, the mechanism behind the HT magnetic order in ZnO is still under debate [4, 5, 6, 7].

Particular attention deserves the role of H doping in ZnO. Hydrogen is a very reactive element that exhibits qualitatively different behaviour in different media. It is amphoteric, can act either as donor (H⁺) or acceptor (H⁻), can occupy different lattice sites and even modify the host structure, and in general counteracts the conductivity of the host. Isolated hydrogen has been found to act as a shallow donor in bulk ZnO, and thus it has been attributed as a source of the unintentional n-type conductivity exhibited by ZnO [8].

At surfaces, the interaction with ambient H is almost unavoidable even in ultra-high-vacuum conditions. Moreover, the presence of hydrogen has a pronounced influence which can even change the surface electronic properties. Understanding the interaction of hydrogen with the ZnO surfaces is crucial in order to control the properties of ZnO-based low-dimensional structures. In recent years, systematic investigations of the different ZnO low-indexed surfaces have been performed [9]. There is agreement in the formation of an ordered hydrogen overlayer on both the non-polar ZnO ($10\bar{1}0$) and the polar O-ended ZnO ($000\bar{1}$) surfaces. Much few work has been devoted to the Zn-terminated ZnO(0001) surface, where the interaction of H atoms is thought to be

the weakest among the ZnO surfaces, since the binding energy of ZnH pairs should be considerably weaker than that of OH bonds. An experimental study revealed that, exposing this surface to atomic hydrogen, an ordered (1×1) overlayer consisting of Zn-hydride species is formed [10]. However, larger exposures to both atomic and molecular hydrogen cause the unexpected unstability of the H (1×1) overlayer, leading to a complete loss of lateral order which reflects a random distribution of H adatoms.

The aim of this Letter is to show that the adsorption of atomic hydrogen on the polar Zn-ZnO(0001) surface gives rise to an ontop H(1×1) ordered overlayer with genuine H-Zn chemical bonds. As shown below, surface magnetism and metallicity are distinct characteristics of this two-dimensional (2D) H(1×1) ordered overlayer. Furthermore, the partial coverage of the surface with H leads to reinforcement of the H-Zn bonds, corrugation of the surface layer and, more interestingly, the emergence of a spin-paired insulating state. Hence, a metal-insulator transition accompanied by the extinction of the magnetization can be driven by reducing the H density on the surface from 1 ML down to 1/2 ML. Further decrease of the H coverage restores the surface metallicity.

Our calculations are based on density functional theory employing norm-conserving pseudopotentials and localized numerical atomic orbitals (AO) as implemented in the SIESTA code[11]. We consider both the local spin density approximation (LSDA) and the generalized gradient approximation (GGA), with the same basis set and parameters of Ref.[5]. Hydrogen is described by a Double Z 1s AO. In order to ensure that our conclusions are robust against the choice of the exchange-correlation functional, we have performed additional total energy optimizations with both the PBE0 and HSE hybrid functionals [12, 13] using the Projector Augmented Wave (PAW) method implemented in the VASP code[14]. We employed similar parameters to those used in Ref. [15],

where such functionals were successfully applied to study the defect energetics in ZnO.

The surfaces are modeled by periodically repeated slabs containing between 15 and 17 atomic planes, separated by a vacuum region of at least 20 Å. Bulk-like behaviour is always attained at the innermost central layers. We calculate both symmetric and asymmetric slabs about the central plane, though we are always subject to the lack of inversion symmetry of the wurtzite structure. We use (1×1) and (2×2) 2D-unit cells to model the surfaces with adsorbed hydrogen. All the atomic positions are allowed to relax until the forces on the atoms are less than 0.03 eV/Å. Brillouin Zone integrations have been performed on a $12 \times 12 \times 1$ Monkhorst-Pack supercell ($12 \times 12 \times 8$ for bulk structures). Careful convergence in the k-mesh and the inclusion of relaxations are essential in order to accurately describe the adsorption states and magnetism.

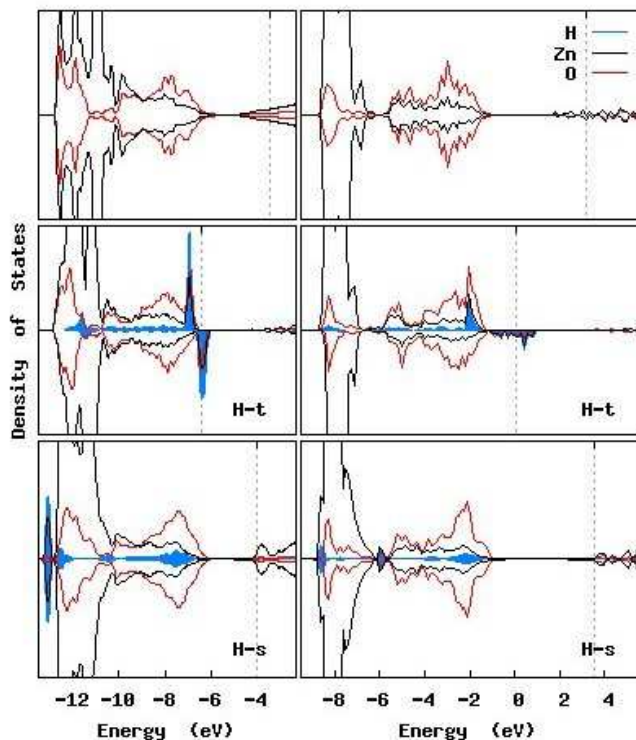


FIG. 1: PDOS projected on the H (filled curve) and neighbouring Zn and O atoms of the (top) bare Zn-Zn(0001) surface, (middle) 1 ML H covered surface, and (bottom) bulk ZnO with a H impurity in the MBC. Left panels correspond to LDA, right ones to HSE.

For 1 ML coverage, the stable adsorption site of H was determined to be atop the Zn atoms after exhaustive minimization considering several surface and subsurface positions, including fcc and hcp hollow, bridge and off-symmetric sites. We present in Figure 1 the density of states projected (PDOS) onto the outermost layers for the bare and H covered surface, both using LDA and

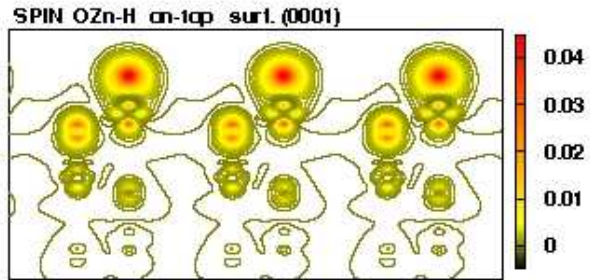


FIG. 2: Side view of the spin density distribution at the ZnO(0001) surface covered by 1 ML H.

the HSE functional. For comparison, the PDOS corresponding to a substitutional H atom at an oxygen site in bulk ZnO -multicenter bonds configuration (MBC) [8]- is also shown. As expected, the HSE functional provides a better description of the band gap and increases the localization of the Zn *d*-states. The calculated gaps using LDA and HSE for bulk ZnO are 0.80 and 3.45 eV, respectively, compared to the experimental value of 3.60 eV. Nevertheless, both calculations provide the same physical picture. The clean surface exhibits the well-known metallic character, with surface states (SS) at the bottom of the conduction band (CB) [16]. However, H adsorption creates hybridized bonding orbitals at the valence band (VB) edge, depleting the Zn 4*s* SS at the CB. The Fermi level lies in the H derived states and thus the surface is metallic and *p*-doped. This is opposite to the bulk MBC, for which the H-bonding state lies deep below the VB with a total charge not large enough to completely deplete the Zn derived CB states.

A distinct characteristic of the H covered surface in the atop geometry is the spin-polarization of the bands. It is not restricted to the H layer, but extends into the ZnO subsurface leading to a net magnetization of the surface region. This is clearly seen in Fig. 2. The magnetic moments at the H, Zn and O layers are 0.29, 0.09 and 0.09 μ_B , respectively, and the magnetic energy gain is around 70 meV. Similar values are obtained in the HSE calculation, the total magnetization differing in less than 10%. Summarizing, H adsorption at the ML coverage gives rise to a *p*-doped metallic surface with the Fermi level pinned at the H-derived bands and a net surface magnetic moment of around 0.5 μ_B .

In order to understand the emergence of the spin polarization when going from the bare Zn surface to the complete H overlayer, we have modelled partial Hydrogen coverages of 3/4, 1/2 and 1/4 MLs with LDA. The corresponding geometric and electronic structures are displayed in Figure 3 and further details are given in Table I. The adsorption of H creates low dispersion states at the

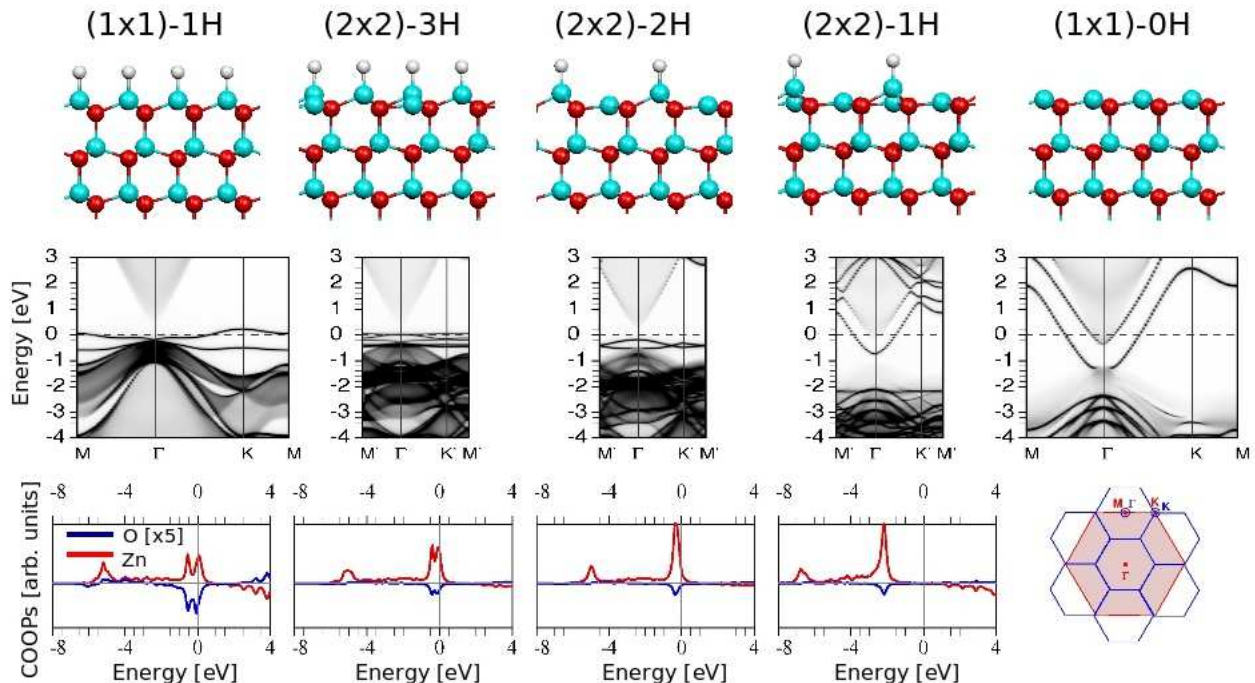


FIG. 3: (Top) Side views of the ZnO(0001) surface for decreasing H coverage from left to right. Oxygen, Zn and H atoms are colored in red, blue and white, respectively. Below each sketch we provide for each case the corresponding: (middle) PDOS projected on the first surface layer and resolved in k -space[17], the BZ for the (1×1) and (2×2) 2D cells being depicted at the right of the bottom panel; (bottom) H-Zn and H-O (magnified by a factor of 5) COOPs.

top of the VB, which are spin-split for 1 ML coverage (with only one spin component completely filled), and start to merge for lower coverages until they become degenerate for $1/2$ ML of H. The main result is that this loss of spin-polarization is accompanied by a metal to insulator transition of the surface. Thus, while at $3/4$ ML the surface is still ferromagnetic and metallic, for a coverage of $1/2$ ML the ground state corresponds to a non-magnetic insulator with the Fermi level above the hydrogen derived band. Further decrease of the hydrogen coverage results in partial occupation of the CB states due to the increased number of unsaturated Zn dangling bonds, restoring the surface metallicity. Therefore, a metal to insulator transition can be tuned by varying the H-coverage back and forth. Even more, by varying the Hydrogen density reversible switch of surface magnetism can be achieved.

A deeper insight about this remarkable phenomenon can be obtained regarding the nature of the bonds -see Table I. In all cases, the H-Zn bond length is significantly shorter than at the bulk ($\sim 2 \text{ \AA}$ in the MBC), a hint of the formation of genuine and stronger chemical bonds at the surface. Furthermore, the bond length reduces as the H coverage diminishes, evidencing a reinforcement of the H-Zn bonds. This bond strengthening is consistent with the variation of the Mulliken charges and the corresponding

TABLE I: H-related surface energy (E_{surf} , in eV), bond distances (d_{AB} , in \AA), and Mulliken charges (Q_A) of the surface atoms for different H coverages and for the bare Zn-ZnO(0001) surface. The last column refers to undoped bulk ZnO.

	1 H	$3/4$ H	$1/2$ H	$1/4$ H	bare	bulk
d_{H-Zn}	1.62	1.60	1.57	1.56		
d_{Zn-O}	0.71	0.78/0.21	0.91/0.20	1.02/0.14	0.39	0.61
Q_H	1.09	1.12	1.17	1.21		
Q_{Zn}	11.36	11.38/11.25	11.42/11.24	11.45/11.27	11.37	11.23
E_{surf}	-1.53	-1.86	-2.51	-3.22		

crystal overlap populations (COOPs) at the lower panel of Figure 3. The charge at both the H and the Zn increases as the H coverage reduces, indicating that a larger amount of charge is shared between the two atoms. The COOPs confirm this scenario, their positive value corresponding to bonding states[18], which are progressively filled as the H coverage reduces. Noticeably, Hydrogen also interacts with the O in the subsurface layer forming an antibonding state.

The reinforcement of the H-Zn bonds can be understood regarding the atomic structures in Figure 3 and Table I. For the clean surface we find a contraction of the first double layer spacing, d_{Zn-O} , in agreement with previous calculations [16]. Contrary, the surface

completely covered with H exhibits a slightly expanded Zn-O distance. For partial H coverages the surface Zn atoms become inequivalent, leading to two different Zn-O interlayer distances and a large corrugation of the Zn plane: those bonded to H experience an outward relaxation while the unbonded ones show an inward relaxation even stronger than that at the bare surface, becoming almost coplanar with the oxygen plane. For deeper layers little relaxation is found. There is a strong correlation between the Zn-O interlayer distance and the redistribution of charge: Zn atoms bonded to H -large $d_{\text{Zn-O}}$ - show an increase in their Mulliken charges, while those not bonded -small $d_{\text{Zn-O}}$ - lose charge approaching the bulk values.

The energies provided in Table I for the H covered surfaces also support the formation of strong bonds with a significant covalent character. They are calculated as the difference between the total energy of the relaxed slab and those of the relaxed isolated ZnO and hydrogen slabs. Their negative values indicate that the chemisorption of hydrogen on the Zn(0001) surface is exothermic. In fact, at a hydrogen density of 1/2 ML the surface energy exceeds by 140 eV the formation of the H_2 molecule in the gas phase, 2.37 eV/H, making adsorbed hydrogen highly stable against desorption. In addition, there is a net reduction of the surface energy for all H coverages with respect to the bare surface. This is specially significant for partial H coverages, where the existence of inequivalent Zn sites allows for the corrugation of the Zn layer and the subsequent decrease of surface energy. These results consistently explain experimental observations, not only about the formation of a $\text{H}(1 \times 1)$ ordered overlayer, but also the loss of surface order under prolonged hydrogen exposures [10]. As shown above, partial H adsorption is energetically more favorable than the bare surface, which could explain the experimentally observed enhancement of the chemical reactivity of surfaces previously exposed to H with respect to the pristine ones. Also the almost coplanar positions of the Zn and O atoms in the bare regions of the partially H covered surface can account for the oxygen signature observed in the XPS spectra [10].

An additional important conclusion can be extracted with respect to the ferromagnetism measured in ZnO, both undoped and doped with magnetic impurities. It has been observed to vary with the oxygen partial pressure, and consequently its existence has been associated to oxygen vacancies. However, calculations as well as careful experiments indicate that oxygen vacancies cannot be a source of magnetism, but instead unsaturated oxygen either due to Zn vacancies or to O-terminated surfaces [5, 6, 7, 19]. Our results strongly suggest that unintentionally adsorbed hydrogen may take active part in the observed magnetism, particularly for undoped ZnO nanocrystals. Adsorbed hydrogen is sensitive to the oxygen partial pressure, since the probability of formation of HO complexes increases with the oxygen chemical po-

tential, leading to the subsequent extinction of the magnetism reported here. Moreover, the hydrogen electron spin has been measured in In_2O_3 when hydrogen acts as an oxygen vacancy passivating center [20].

As a final remark, the Zn-ZnO(0001) surface may undertake a triangularly shaped reconstruction under specific growth conditions [21]. We have investigated the effect of such reconstruction through calculations of stepped surfaces, and the general conclusions are analogous to those presented here for the unreconstructed surface, although strong O-H bonds are also formed at step edges.

In summary, atomic hydrogen adsorbs on the Zn-ZnO(0001) polar surface atop the Zn atoms, forming strong H-Zn bonds and leading to a metallic, *p*-doped surface with a net magnetic moment. As the H coverage diminishes, there is a reinforcement of the remaining H-Zn bonds accompanied by the removal of the valence band holes and the subsequent extinction of magnetism. We predict that controlling the Hydrogen coverage can serve to tune a metal-insulator transition and to achieve reversible switch of surface magnetism.

We are indebted to Prof. P. Esquinazi and Prof. N. García for fruitful discussions. We also acknowledge the unvaluable support of Dr. C. Francini and Prof. J. Häfner in the calculations using hybrid functionals. This work was supported by the Spanish Ministry of Science and Technology (MAT2006-05122).

* Electronic address: mcarmen@icmm.csic.es

- [1] Ü. Ozgur *et al.*, J. Appl. Phys. **98**, 041301 (2005).
- [2] K. Ueda, H. Tabedo, and T. Kawai, Appl. Phys. Lett. **79**, 988 (2001).
- [3] D.D. Awschalom, and M.E. Flatté, Nature. Phys. **3**, 153 (2007).
- [4] S.A. Chambers, and B. Gallagher, New J. Phys. **10** (2008), articles: 055004-055018.
- [5] N. Sanchez, S. Gallego, and M.C. Muñoz, Phys. Rev. Lett. **101**, 067206 (2008).
- [6] A. Sundaresan *et al.*, Phys. Rev. B **74**, 161306(R) (2006).
- [7] Q. Xu *et al.*, Appl. Phys. Lett. **92**, 082508 (2000).
- [8] C.G. Van de Walle, Phys. Rev. Lett. **85** 1012 (2000); A. Janotti, and C.G. Van de Walle, Nature materials **6**, 44 (2007).
- [9] C. Wöll, Progress in Surf. Sci. **82**, 55 (2007), and references therein.
- [10] T. Becker *et al.*, Surf. Sci. **486**, L592 (2001); **511**, 463 (2002).
- [11] J.M. Soler *et al.*, J. Phys.: Condens. Matter **14**, 2745 (2002).
- [12] The PAW data sets with radial cutoffs of 1.3, 0.9, and 0.4 Å for Zn, O, and H, respectively, were used with a plane-wave cutoff energy of 350 eV. The HSE functional was built using a 0.38 fraction of exact exchange and a screening parameter of 0.2 Å⁻¹.
- [13] J. Paier *et al.*, J. Chem. Phys. **124**, 154709 (2006), and

references therein.

- [14] G. Kresse, and J. Hafner, Phys. Rev. B **47**, 558(R) (1993); G. Kresse, and J. Furthmüller, Phys. Rev. B **54**, 11169 (1996); G. Kresse, and D. Joubert, Phys. Rev. B **59**, 1758 (1999).
- [15] F. Oba *et al.*, Phys. Rev. B **77**, 245202 (2008).
- [16] G. Kresse, O. Dulub, and U. Diebold, Phys. Rev. B **68**, 245409 (2003).
- [17] C. Rogero *et al.*, Phys. Rev. B **69**, 045312 (2004).
- [18] J.I. Beltrán *et al.*, Phys. Rev. B **68**, 075401 (2003).
- [19] H. Peng *et al.*, Phys. Rev. Lett. **102**, 017201 (2009).
- [20] M. Kumar *et al.*, Appl. Phys. Lett. **95**, 13102 (2009).
- [21] O. Dulub, U. Diebold, and G. Kresse, Phys. Rev. Lett. **90**, 016102 (2003).